Appl Microbiol Biotechnol (2015) 99:3081–3091
DOI 10.1007/s00253-014-6148-y

Structural basis for the 4′-hydroxylation of diclofenac by a microbial cytochrome P450 monooxygenase

Lian-Hua Xu · Haruo Ikeda · Ling Liu · Takatoshi Arakawa · Takayoshi Wakagi · Hirofumi Shoun · Shinya Fushinobu

Received: 18 August 2014 / Revised: 6 October 2014 / Accepted: 9 October 2014 / Published online: 24 October 2014

Abstract Diclofenac is a nonsteroidal anti-inflammatory drug. It undergoes hydroxylation by mammalian cytochrome P450 enzymes at 4′- and/or 5′-positions. A bacterial P450 enzyme, CYP105D7 from *Streptomyces avermitilis*, has been shown to catalyze hydroxylation of 1-deoxypentalenic acid and an isoflavone daidzein. Here, we demonstrated that CYP105D7 also catalyzes hydroxylation of diclofenac at the C4′-position. A spectroscopic analysis showed that CYP105D7 binds diclofenac in a slightly cooperative manner with an affinity of 65 μM and a Hill coefficient of 1.16. The crystal structure of CYP105D7 in complex with diclofenac was determined at 2.2 Å resolution. The distal pocket of CYP105D7 contains two diclofenac molecules, illustrating drug recognition with a double-ligand-binding mode. The C3′ and C4′ atoms of the dichlorophenyl ring of one diclofenac molecule are positioned near the heme iron, suggesting that it is positioned appropriately for aromatic hydroxylation to yield the 4′-hydroxylated product. However, recognition of diclofenac by CYP105D7 was completely different from that of rabbit CYP2C5, which binds one diclofenac molecule with a cluster of water molecules. The distal pocket of CYP105D7 contains four arginine residues, forming a wall of the substrate-binding pocket, and the arginine residues are conserved in bacterial P450s in the CYP105 family.

L.-H. Xu (✉) · L. Liu
Ocean College, Zhejiang University, 866 Yuhangtang Road, Hangzhou, Zhejiang 310058, China
e-mail: lianhuaxu@zju.edu.cn

H. Ikeda
Kitasato Institute for Life Sciences, Kitasato University, 1-15-1 Kitasato, Sagamihara, Kanagawa 252-0373, Japan

T. Arakawa · T. Wakagi · H. Shoun · S. Fushinobu (✉)
Department of Biotechnology, Graduate School of Agriculture and Life Sciences, The University of Tokyo, 1-1-1 Yayoi, Bunkyo-ku, Tokyo 113-8657, Japan
e-mail: asfushi@mail.ecc.u-tokyo.ac.jp

Keywords Diclofenac · Cytochrome P450 · X-ray crystallography · *Streptomyces avermitilis* · Xenobiotics

Introduction

Cytochrome P450s (CYP or P450) catalyze a wide range of xenobiotics and endogenous compounds such as pollutants, environmental compounds, and drug molecules as well as biosynthetic reactions involving sterols, fatty acids, prostaglandins, and antibiotics (Lamb et al. 2007; Ortiz de Montellano 2005). Microbial P450s (especially those from *Streptomyces* strains) have practical advantages for biotechnical applications because of their variety and stability (Bernhardt and Urlacher 2014; Lamb et al. 2013).

The CYP105 family has been extensively investigated and characterized because this family has crucial roles in xenobiotic degradation and the biosynthesis of antibiotics (Sawada et al. 2004; Serizawa and Matsuoka 1991; Xu et al. 2010). The CYP105D subfamily is particularly interesting because of its detoxifying role in soil, whereby bacteria may be exposed to toxic secondary metabolites from live organisms and decay organic material (Lamb et al. 2002). For example, CYP105D1 (P450soy) from *Streptomyces griseus* metabolizes a diverse array of structurally complex xenobiotics from sources such as pharmaceuticals, agrochemicals, and environmental pollutants (Taylor et al. 1999). CYP105D5 from *Streptomyces coelicolor* metabolizes testosterone and fatty acids (Agematu et al. 2006; Chun et al. 2007).

Recently, CYP105D7 from *Streptomyces avermitilis* was shown to be responsible for the production of a shunt metabolite in the biosynthesis of the pentalenolactone family of antibiotics by hydroxylation of 1-deoxypentalenic acid at the C-1 position (Takamatsu et al. 2011). CYP105D7 also catalyzes hydroxylation of the isoflavone daidzein at the 3′-position (Pandey et al. 2010). Although many P450 genes were

found from genome sequences of Actinomycetales microorganisms at the average of 10 to 20 genes per genome, biochemical function of their gene products was still unknown except those in biosynthetic gene cluster for secondary metabolites. We have been evaluating the function of actinomycete P450s through conversion of many compounds including natural products using recombinant proteins, and some P450s had the ability to hydroxylate the compounds, which are known to be hydroxylated by human P450s. In our preliminary study, CYP105D7 catalyzed hydroxylation of many compounds, including diclofenac, tolbutamide, testosterone, compactin, and so on. Out of these compounds, diclofenac was the most suitable substrate for the hydroxylation reaction of CYP105D7 (H. Ikeda et al., unpublished data).

Diclofenac (Fig. 1) is a nonsteroidal anti-inflammatory drug advocated for use in painful and inflammatory rheumatic as well as certain nonrheumatic conditions (Todd and Sorkin 1988). Diclofenac is hydroxylated in a highly regioselective manner at the 4′-position by human CYP2C9 and rabbit CYP2C5 (Mancy et al. 1999). In contrast, other human CYP2C enzymes such as 2C8, 2C18, and 2C19 produce mixtures of 4′- and 5-hydroxydiclofenac (Mancy et al. 1999; Wester et al. 2003), and CYP3A4 produces 5-hydroxydiclofenac (Shen et al. 1999). Moreover, a recent study suggested that diclofenac inhibits human CYP1A2 in vivo (Ohyama et al. 2014). With respect to bacterial P450s, CYP107E4 from *Actinoplanes* sp. ATCC 53771 and the D251G/Q307H double mutant of P450BM3 (CYP102A1) from *Bacillus megaterium* catalyze the 4′-hydroxylation of diclofenac (Prior et al. 2010; Tsotsou et al. 2012). However, the structural basis for the hydroxylation of diclofenac by P450s has been clarified only for rabbit CYP2C5 (Wester et al. 2003).

Previously, we reported on the crystal structures of the CYP105P1–filipin I complex and substrate-free state of CYP105D6. CYP105P1 and CYP105D6 are involved in the biosynthesis of the filipin gene cluster by catalyzing regiospecific and stereospecific hydroxylations at positions C26 and C1′, respectively (Xu et al. 2010). CYP105D7 and CYP105D6 belong to the same subfamily and share 56 % amino acid sequence identity, but their substrate specificities are completely different.

Here, we show that CYP105D7 catalyzes the 4′-hydroxylation of diclofenac. Moreover, we describe the crystal

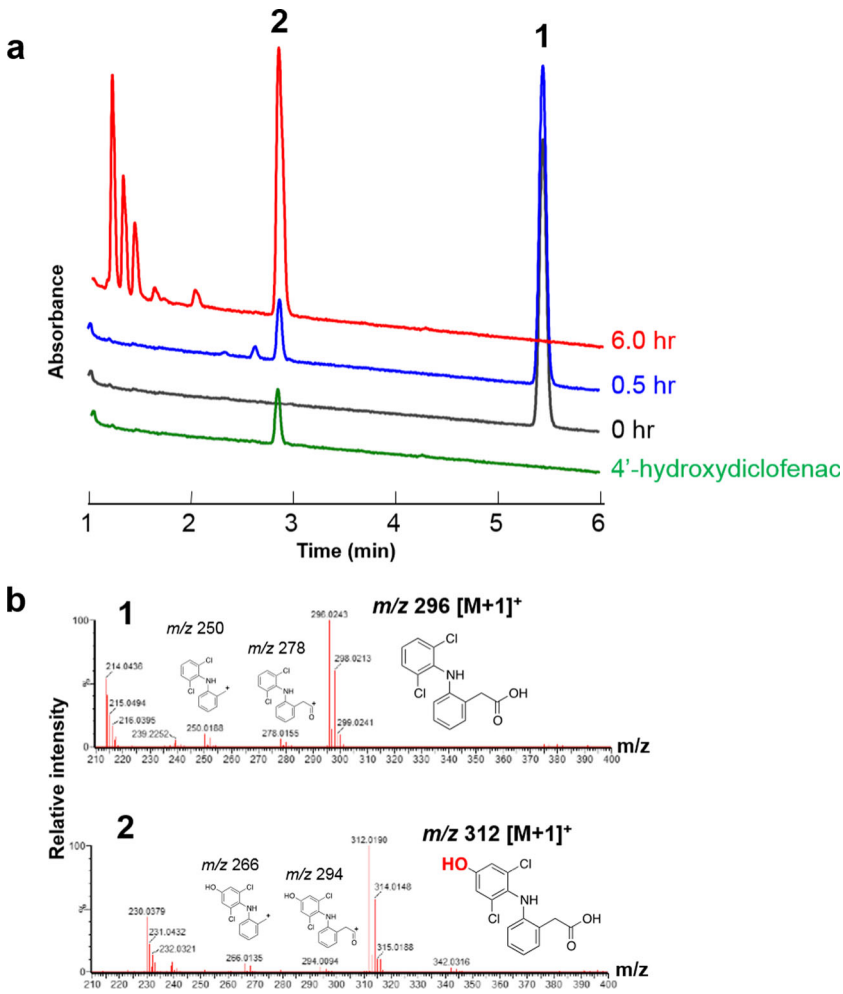

Fig. 1 Conversion of diclofenac by *E. coli* BL21 (DE3) carrying pET17*::sav7469::camA-camB*. **a** HPLC-MS analysis of conversion products extracted at 0-, 0.5-, and 6-h incubation. The lowest chromatogram indicates an authentic sample of 4′-hydroxydiclofenac (2.8 min). **b** Time of flight mass spectrometry (TofMS) spectra of samples eluted at 5.4 min of 0.5-h incubation (*1*) and at 2.8 min of 6.0-h incubation (*2*), respectively

structure of CYP105D7 in complex with diclofenac, providing the structural basis for the "ligand promiscuity" and molecular recognition of diclofenac for this hydroxylation.

Materials and methods

Construction of a CYP105D7 coexpression system

A gene (*sav7469*) encoding CYP105D7 was amplified by the polymerase chain reaction (PCR) with template DNA from a cosmid CL_228_E11 (http://avermitilis.ls.kitasato-u.ac.jp) using the primer pair forward 5′-GCCCATATGACAGAG CCCGGTACGTCCGTG-3′ (underlined and bold characters indicate the *Nde*I site and transcriptional start codon, respectively) and reverse 5′-GCACTAGTTCAGCTTGCC GACCGCGGGAC-3′ (underlined characters indicate the *Spe*I site). The PCR program employed was the following: initial denaturation step (95 °C, 2 min) followed by 30 cycles of amplification (95 °C for 30 s, 58 °C for 30 s, and 72 °C for 70 s) and then a final incubation at 72 °C for 5 min. The resulting amplicon was digested with *Nde*I, *Spe*I, and *Dpn*I (removal of template DNA). The plasmid pT7NS-camAB (Fujita et al. 2009), whose *camA* and *camB* genes encode the putidaredoxin reductase and puridaredoxin of the *Pseudomanas putida* plasmid, was double-digested with *Nde*I and *Spe*I. These two digested PCR products were ligated. The ligation mixture was used to transform the competent cells of *Escherichia coli* DH5α. The resultant recombinant plasmid, pET11::*sav7469::camA-camB*, was isolated from cultures grown on Luria–Bertani (LB) medium containing 50 μg/mL of ampicillin. After the region of *sav7469* in the recombinant plasmid was confirmed by sequence analyses, the plasmid was transformed into *E. coli* BL21 (DE3) for the study of expression. Transformants of *E. coli* BL21 (DE3) carrying pET11::*sav7469::camA-camB* were grown in LB medium containing 50 μg/mL of ampicillin with shaking at 37 °C for 18 h. A 0.1-mL portion of the culture was inoculated into 10 mL of M9 medium (M9 salts, 1 % casamino acids, 0.4 % glucose, 0.1 mM $CaCl_2$, 1 mM $MgCl_2$, 0.1 mM $FeCl_3$, and 50 μg/mL of ampicillin), and the culture incubated with shaking at 37 °C until the optical density at 600 nm (OD_{600}) reached 0.8. Then, isopropyl β-D-thiogalactopyranoside (IPTG) and 5-aminolevulinic acid were added to final concentrations of 0.1 and 0.5 mM, respectively, and cultivation continued for further 20 h at 22 °C. Cells were collected by centrifugation at 3,000 rpm for 10 min at 4 °C. Sedimented cells were washed with 5 mL of buffer containing 50-mM potassium phosphate buffer, pH 7.2, 1 mM ethylenediaminetetraacetic acid (EDTA), 2 mM dithiothreitol (DTT), and 10 % (*v*/*v*) glycerol. Washed cells were suspended in 1 mL of the same buffer.

Bioconversion of diclofenac and high-performance liquid chromatography–time-of-flight–mass spectrometry (HPLC-TOF-MS) analyses

Hydroxylation of diclofenac was undertaken by bioconversion using a 0.5-mL suspension of IPTG-induced *E. coli* carrying pET11*::sav7469::camA-camB* in the presence of 0.15 mM diclofenac. The reaction mixture was incubated with gentle shaking at 30 °C for 0, 0.5, and 6 h. The reaction was stopped by addition of 0.5 mL of acetonitrile. The supernatant was collected by centrifugation at 15,000 rpm for 5 min at room temperature. A 2-μL portion of the supernatant was analyzed directly by HPLC-TOF-MS (Acquity UPLC System, Xevo G2-S TOF; Waters, Milford, MA, USA). Analytical conditions for HPLC were the following: column, UPLC BEH C-18 (1.7 μm; 2.1 mm×50 mm); mobile phase, 30–60 % acetonitrile in 0.05 % (*v*/*v*) formic acid for 6 min; flow rate, 0.2 mL/min; detection at 275 nm. Mass spectrometry was done in resolution mode under the following conditions: capillary voltage of 3.0 kV in positive ion mode; cone voltage of 40 V; source temperature of 120 °C; desolvation gas flow of 800 L/h at 450 °C; cone gas flow of 50 L/h. For accurate mass measurements, lock mass calibration was conducted using leucine–enkephalin. Mass data were acquired with collision cell energy alternating between low energy (6 V) and elevated energy (ramping from 20 to 40 V). An authentic sample of 4′-hydroxydiclofenac was purchased from Sigma-Aldrich Japan (Tokyo, Japan).

Heterologous expression and purification of CYP105D7

CYP105D7 protein with a 4-His tag at the C-terminus was expressed and purified as described (Takamatsu et al. 2011). CYP105D7 with no His tag at the C-terminus was expressed with a similar method and purified to homogeneity by sequential column chromatography involving Q Sepharose FF, Hydroxyapatite, Resource Q, and Hiload 16/600 Superdex 200 (GE Healthcare, Piscataway, NJ, USA). The purified enzyme with or without the His tag appeared as a single band corresponding to a molecular mass of 45 kDa on sodium dodecyl sulfate–polyacrylamide gel electrophoresis. The absorbance ratio of proteins purified in this manner was >2.0 at 420 nm as compared with that at 280 nm. P450 content measured by carbon monoxide (CO) difference spectroscopy (Omura and Sato 1964) was also undertaken to verify purification quality (data not shown).

Spectroscopy

Purified CYP105D7 with a 4-His tag at C-terminus was used for a spectroscopic analysis. Diclofenac (sodium salt) was purchased from Wako Pure Chemicals (Osaka, Japan). Measurements of ultraviolet (UV) visible absorption spectra and titration experiments were undertaken using essentially the

same methods as described previously (Xu et al. 2009). For titrations of diclofenac to CYP105D7, 1 mL of assay buffer containing 50 mM potassium phosphate (pH 7.5), 0.1 mM DTT, 0.1 mM EDTA, and 10 % (*v*/*v*) glycerol was used. A nonlinear fitting with a Hill equation was applied to determine the binding constants using Kaleidagraph (Synergy, Reading, PA):

$$\Delta A = \frac{B_{max}[L]^{n_H}}{[K_A]^{n_H} + [L]^{n_H}}$$

B_{max} is the maximum absorbance difference extrapolated to infinite ligand enzyme concentration, K_A is the half-maximal binding constant, n_H is the Hill coefficient, and L is the ligand concentration.

Crystallography

For crystallization, the CYP105D7 protein without the 4-His tag was used. The protein was concentrated to >20 mg/mL in 10 mM Tris–HCl (pH 7.5), 0.1 mM EDTA, 0.1 mM DTT, and 10 % (*v*/*v*) glycerol. Crystallization was done using the sitting-drop vapor diffusion method. Various screening kits, such as Crystal Screen, Crystal Screen 2, PEG/ion, JCSG Core I, II, JCSG+ Suite, Wizard III, IV, and Precipitant Synergy, were used for the initial search. Crystals grew in several conditions from PEG/Ion, JCSG+ Suite, and Precipitant Synergy kits. After optimizing the conditions of salt, pH, precipitant, and temperature and using Additive Screen kit, suitable crystals were obtained. Crystals of the diclofenac-bound form were grown at 20 °C by mixing 1 μL of the protein solution (15 mg of protein/mL and 2 mM diclofenac) and 0.8 μL of the reservoir solution comprising 0.2 M sodium chloride, 0.1 M Na/K phosphate (pH 5.5), 48 % PEG200, and 0.2 μL 40 % tert-butanol. X-ray diffraction data were collected using a charged couple device camera at the BL-17A station at the Photon Factory, High Energy Accelerator Research Organization (KEK), Tsukuba, Japan. Without cryoprotection, crystals were flash-cooled directly in a nitrogen stream at 100 K. Diffraction images were processed using the HKL2000 program suite (Otwinowski and Minor 1997). The structure was solved by molecular replacement using MOLREP (Vagin and Teplyakov 1997). The search model was prepared using the homology modeling server 3D-JIGSAW (Bates et al. 2001) based on the structure of CYP105A1 (Sugimoto et al. 2008). Manual model rebuilding, introduction of water molecules, and refinement were performed using Coot (Emsley et al. 2010) and Refmac5 (Murshudov et al. 1997). Data collection and refinement statistics are shown in Table 1. Figures were prepared using PyMol (Schrödinger, Portland, OR, USA). The coordinates and structure factors have been deposited in the PDB under accession codes 4UBS.

Table 1 Data collection and refinement statistics

Data set	CYP105D7–diclofenac complex
Data collection statistics	
Wavelength (Å)	0.980
Space group	$P3_121$
Unit cell (Å)	$a=b=139.877$
	$c=65.268$
Resolution (Å)[a]	50.00–2.20
	(2.24–2.20)
Total reflections	402,802
Unique reflections	37,612
Completeness (%)[a]	99.2 (100.0)
Redundancy[a]	10.8 (11.1)
Mean $I/\sigma(I)$[a]	32.9 (4.4)
R_{merge} (%)[a]	8.4 (62.3)
Refinement statistics	
Resolution range (Å)	44.40–2.20
No. of reflections	35,399
R factor/R_{free} (%)	17.7/22.8
No. of atoms	3582
Average B factor (Å^2)	
Protein	40.3
Heme	28.5
DIF	42.3
PGE	60.4
PEG	71.5
Water	50.7
PO_4	67.4
RMSD from ideal values	
Bond lengths (Å)	0.019
Bond angles (°)	2.134
Ramachandran plot (%)[b]	
Favored	97.4
Allowed	2.6
Outlier	0

[a] Values in parentheses are for the highest resolution shell

[b] Determined by RAMPAGE server (Lovell et al. 2003)

Results

Conversion of diclofenac to 4′-hydroxydiclofenac by a CYP105D7 coexpression system

Catalytic activity of P450s must be associated with redox partner proteins that transfer electrons from NAD(P)H to the P450 heme center (Urlacher and Girhard 2012). Bacterial P450 systems comprise a small redox 2Fe–2S ferredoxin and a flavin adenine dinucleotide-containing reductase. Hydroxylation of diclofenac by CYP105D7 (SAV_7469)

was done using a resting cell system prepared by IPTG-induced *E. coli* transformant carrying *sav7469*, *camA*, and *camB*. Formation of hydroxylated diclofenac was analyzed by HPLC-TOF-MS (Fig. 1). HPLC analyses showed that the retention time of the product was 2.8 min, which is identical to that of an authentic 4′-hydroxydiclofenac (Fig. 1a). When we mixed the reaction product and the authentic sample, they eluted in the same peak on the HPLC analysis. The retention times of the product and the authentic 4′-hydroxydiclofenac sample were always identical under all solvent conditions we tested (data not shown). TOF-MS analyses of the product peak clearly indicated a monohydroxylated product with a mass of *m/z* 312 $[M+1]^+$ (Fig.1b). About 20 % of diclofenac (*m/z* 296 $[M+1]^+$) was converted to the monohydroxylated compound (*m/z* 312 $[M+1]^+$) at 0.5 h of incubation. Diclofenac in the reaction mixture was converted completely to the monohydroxylated compound at 6 h of incubation. A fragmentation pattern of the monohydroxylated product was identical to that of the authentic 4′-hydroxydiclofenac sample. Thus, we concluded that CYP105D7 catalyzes the hydroxylation at the 4′-position of diclofenac.

Spectroscopic characterization

Recombinant protein of CYP105D7 with a 4-His tag at the C-terminus was expressed in *E. coli* cells and purified to homogeneity. A basic spectroscopic characterization of the purified CYP105D7 (including measurements of the UV–Visible absorption spectra of oxidized, reduced, and CO-bound forms) has been described (Takamatsu et al. 2011). Figure 2 shows a spectral titration result of CYP105D7 with diclofenac. The spectral change of CYP105D7 illustrated a typical type I shift of the Soret peak from 419 (low spin) to 394 nm (high spin), suggesting that the water molecule coordinated as the sixth ligand of heme in the resting state was removed completely by diclofenac binding. This result was in accordance with the crystal structure of the diclofenac complex (discussed below). The binding curve was slightly sigmoidal, and analysis of the data by using the Hill equation yields a Hill coefficient (n_H) of 1.16±0.05 and half-maximal binding (K_A) at 65±5 μM. This result indicates that the binding of diclofenac to CYP105D7 was slightly cooperative, as in the case of P450eryF with androstenedione and 9-aminophenanthrene (Cupp-Vickery et al. 2000).

CYP105D7–diclofenac complex

Crystallization experiments using the recombinant protein of CYP105D7 with the C-terminal 4-His tag were not successful, but a construct without the His-tag was crystallized with good reproducibility. Diffraction data were collected using a crystal grown with 1.1 mM diclofenac. The crystal structure of CYP105D7 was determined at a resolution of 2.2 Å and was

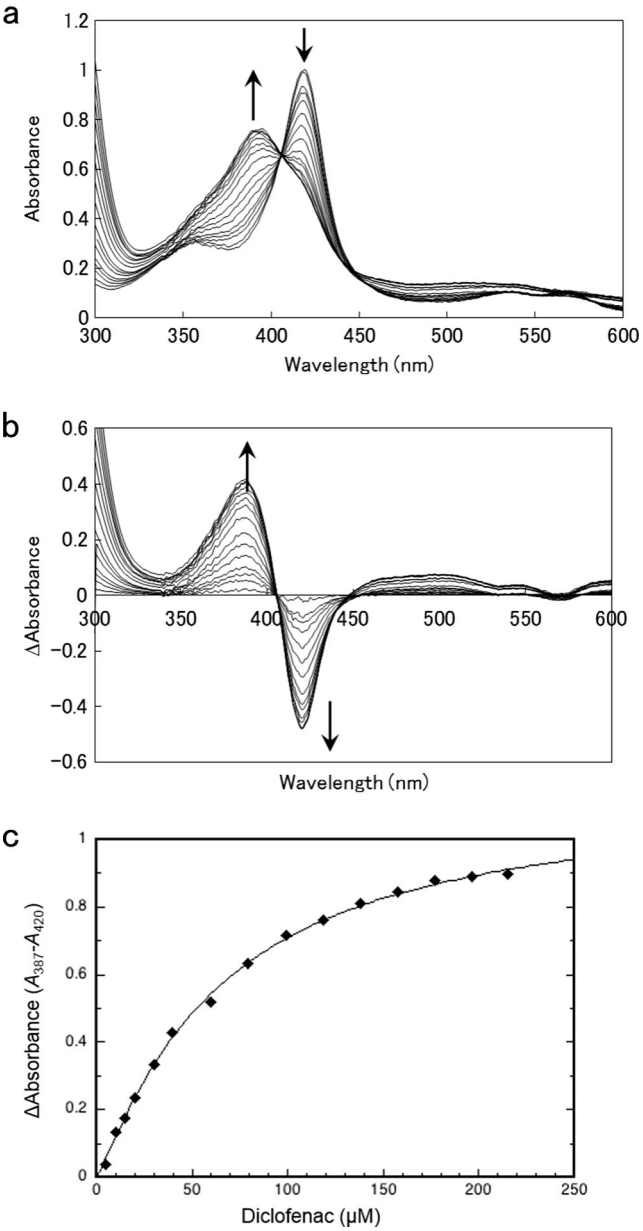

Fig. 2 Spectral changes of CYP105D7 (ferric resting state) upon addition of increasing concentrations of diclofenac (**a**), its difference spectra (**b**), and the titration curve calculated using the values of absorption differences at 387 and 420 nm (**c**). *The solid line* is a nonlinear regression fitting of the experimental points to the Hill equation

refined to an *R* factor of 17.7 % (R_{free}=22.8 %). The crystal contains one molecule in the asymmetric unit and exhibits a relatively high Matthews coefficient (4.08 $Å^3$/Da) and solvent content (69.9 %). Figure 3a shows the overall structure of CYP105D7 in complex with diclofenac. CYP105D7 has a typical P450 fold, being composed of 13 α-helices (A-L) and 6 β-sheets. The BC loop region and the FG helices, which often adopt an open–close motion on ligand binding (Munro et al. 2013), are in a closed conformation. The final model contains residues from Ala10 to Trp402, including one heme, two diclofenac molecules (DIF-1, DIF-2), five triethylene

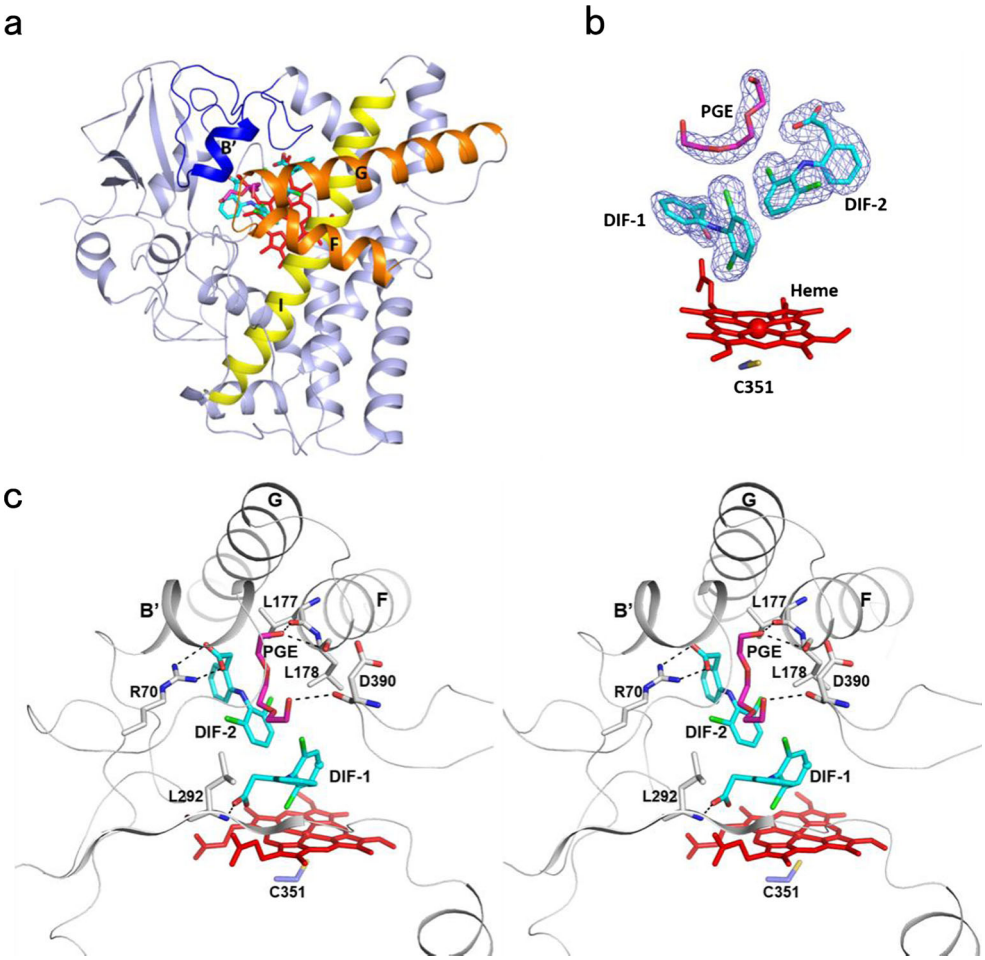

Fig. 3 **a** Overall structure of the CYP105D7–diclofenac complex. The BC loop, FG loop region, and I helix are shown in *blue*, *orange* and *yellow*, respectively. Heme, diclofenac, and triethylene glycol (PGE) molecules are shown as *red*, *cyan*, and *magenta sticks*, respectively. **b** F_{obs}–F_{calc} omit electron density map of the diclofenac and PGE molecules contoured at 3.0 σ. Cys351 is shown as *blue stick*. **c** Stereographic diagram showing interactions with the BC loop, FG helices, and β6 sheet regions. Amino acid residues involved in ligand recognition are shown as *sticks*. Hydrogen bonds are shown as *dotted lines*. Distances between the C3′ and C4′ atoms of DIF-1 with heme iron are 4.9 and 6.2 Å, respectively

glycol (PGE) molecules, 14 di(hydroxyethyl)ether (PEG) molecules, 304 water molecules, and one phosphate ion. A structural similarity search using the DALI server (Holm and Sander 1995) suggested that CYP105D7 shows high similarity to the (1α,25(OH)$_2$D$_3$)-bound form of CYP105A1 R73A/R84A mutant (PDB code 3CV9 chain A; Z score=59.7; root-mean square deviation (RMSD) for 394 Cα atoms=1.2 Å) (Hayashi et al. 2008), NAAD-bound form of P450nor S73G/S75G mutant (PDB code 1XQD chain A; Z score=52.1; RMSD for 392 Cα atoms=1.7 Å) (Oshima et al. 2004), and filipin I-bound form of CYP105P1 (PDB code 3ABA; Z score=50.4; RMSD for 387 Cα atoms=2.0 Å) (Xu et al. 2010). Volumes of the substrate-binding pockets were calculated using the CASTp server with probe radius of 1.4 Å (Dundas et al. 2006). The pocket volume of CYP105D7 is 2,037 Å^3, so was large enough to accommodate the two diclofenac molecules. The volume size is similar to that of CYP105P1 (PDB 3ABA) (2,166 Å^3), which contains the large macrolide substrate filipin I (Xu et al. 2010).

The electron density map for two diclofenac molecules (DIF-1, DIF-2) and one PGE molecule was observed in the distal (active site) pocket (Fig. 3b). The double binding mode of diclofenac is consistent with its slightly cooperative binding on the spectroscopic analysis (Fig. 3c). The proximal ligand, DIF-1, was positioned almost parallel to the heme, and the plane of its dichlorophenyl ring was perpendicular to that of the heme. The carboxyl group of DIF-1 was hydrogen-bonded with the backbone amino group of Leu292, which is located in the β6 strand (Fig. 3c). The dichlorophenyl ring of DIF-1 is located near the heme group, with its C3′ and C4′ atoms positioned 4.9 and 6.2 Å from the heme iron, respectively. This observation suggests that these atoms are located appropriately for aromatic hydroxylation (discussed below). The two diclofenac and PGE molecules are located in a predominantly hydrophobic pocket formed by the heme, BC loop, FG helix, I helix, K/β6 strand region, and C-terminal loop regions (Fig. 4a). Residues recognizing the DIF-1 molecule are Leu93 (BC loop), Leu178 (FG helices), Ala241 and Thr245 (I helix), Ala288, Asp289, Gly290, Leu291, Leu292 (K/β6 strand), and Ile392 (C-terminal loop). In particular, the β6 strand and the previous loop region form a small pocket for the phenylacetic acid ring. The DIF-2 molecule was located above DIF-1 and bound in the middle of the distal pocket. DIF-2 was inclined at ≈45° from the vertical axis of the heme plane. The carboxyl group of DIF-2 forms a salt bridge with the guanidinium group of Arg70 in the B/B′ loop. The distance between the

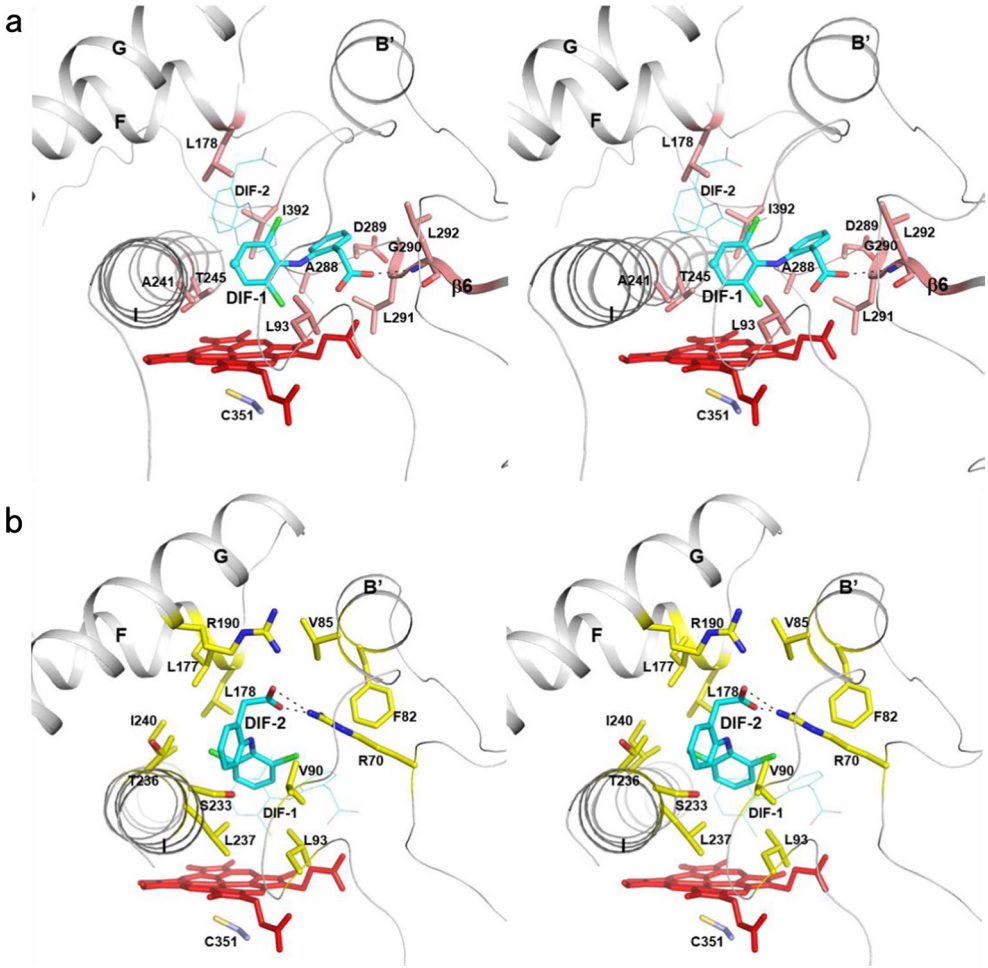

Fig. 4 Stereographic diagrams showing DIF-1 (**a**) and DIF-2 (**b**) recognition. Diclofenac, Cys351, and heme are shown as *cyan*, *blue*, and *red sticks*, respectively. The hydroxylation target position, C4′ of DIF-1, is shown as *sphere*. Amino acid residues recognizing DIF-1 (**a**) and DIF-2 (**b**) are shown as *salmon* and *yellow sticks*, respectively

C4′ atom of DIF-2 and heme iron is 8.0 Å, suggesting that the DIF-2 molecule is not hydroxylated but has a role in stabilizing DIF-1 binding. Residues recognizing the DIF-2 molecule are Arg70, Phe82, Val85, Val90, Leu93 (BC loop), Leu177, Leu178, Arg190 (FG helices), Ser233, Thr236, Leu237, and Ile240 (I helix) (Fig. 4b). A PGE molecule that originated from the crystallization precipitant was identified as the third molecule in the distal pocket. It is positioned at the entrance of the distal pocket and was hydrogen-bonded with the backbone carbonyl groups of Leu177 and Asp390. The PGE molecule is an artifact of crystallization, but its presence suggests that the distal pocket of CYP105D7 has room for a third long molecule in addition to the two diclofenac molecules.

Multiple ligand-binding mode of P450s

The distal pocket of the CYP105D7–diclofenac structure simultaneously contains two diclofenac molecules and one PGE molecule. The double-ligand-binding mode was first reported for a bacterial P450, P450eryF from *Saccharopolyspora erythraea* (CYP107A1), in complex with androstenedione and 9-aminophenanthrene (Cupp-Vickery et al. 2000). The spectroscopic binding analysis of these compounds on P450eryF also exhibited cooperative bindings with Hill coefficients of 1.31 and 1.38. Similar structures containing multiple ligands in the distal pocket have been reported, especially for mammalian P450s responsible for drug metabolism with wide substrate specificities. In the case of CYP3A4, two ketoconazole molecules have been observed in the distal pocket of the complex structure (Ekroos and Sjögren 2006). In addition, the double-ligand-binding mode has been observed in CYP2C8 in complex with 9-*cis*-retinoic acid (Schoch et al. 2008), CYP2A13 in complex with tobacco procarcinogen 4-(methylnitrosamino)-1-(3-pyridyl)-1-butanone (NNK) (DeVore and Scott 2012), and bovine CYP21A2 in complex with 7-hydroxyprogesterone (17OHP) (Zhao et al. 2012a). The distal binding site of the two-binding mode can be recognized as an "antechamber" site (Johnson and Stout 2013). In a crystal structure of CYP2C9 (PDB code 1OG5), an antechamber site was occupied by an *S*-warfarin molecule, whereas the functional (proximal to heme) site is unliganded (Williams et al. 2003). The antechamber site of CYP2C9 was speculated to serve as an effector site or as an initial binding site.

Discussion

In the mammalian liver, diclofenac is converted mainly to 4′-hydroxydiclofenac by CYP2C5 or CYP2C9 (Mancy et al. 1999). Among them, the crystal structure of rabbit CYP2C5 in complex with diclofenac has been reported (PDB code 1NR6) (Wester et al. 2003). Superimposition of the active sites of CYP105D7–diclofenac and CYP2C5–diclofenac is shown in Fig. 5a. The proximal diclofenac molecule in CYP105D7 (DIF-1) is not aligned well with the diclofenac molecule in CYP2C5, but their dichlorophenyl rings are located near the heme iron. The C3′ and C4′ atoms of the diclofenac in CYP2C5 are in the closest position to the heme iron with distances of 4.4 and 4.7 Å, respectively. In the case of CYP105D7, the C3′ atom (4.9 Å) is more proximal to the heme iron than the C4′ atom (6.2 Å). These orientations are in accordance with a mechanism for aromatic hydroxylation involving formation of a 3′-4′ epoxide intermediate that finally rearranges to yield the 4′-hydroxylated diclofenac (Guengerich 2003). In the CYP2C5 structure, the carboxyl moiety of diclofenac is extensively hydrogen-bonded by a cluster of water molecules held by the side chains of Asn204, Lys241, and Asp290. In contrast, in CYP105D7 structure, the carboxyl moiety of the distal diclofenac (DIF-2) forms a direct salt bridge with Arg70 in the B/B′ loop. This binding mode is similar to the flurbiprofen complex structure

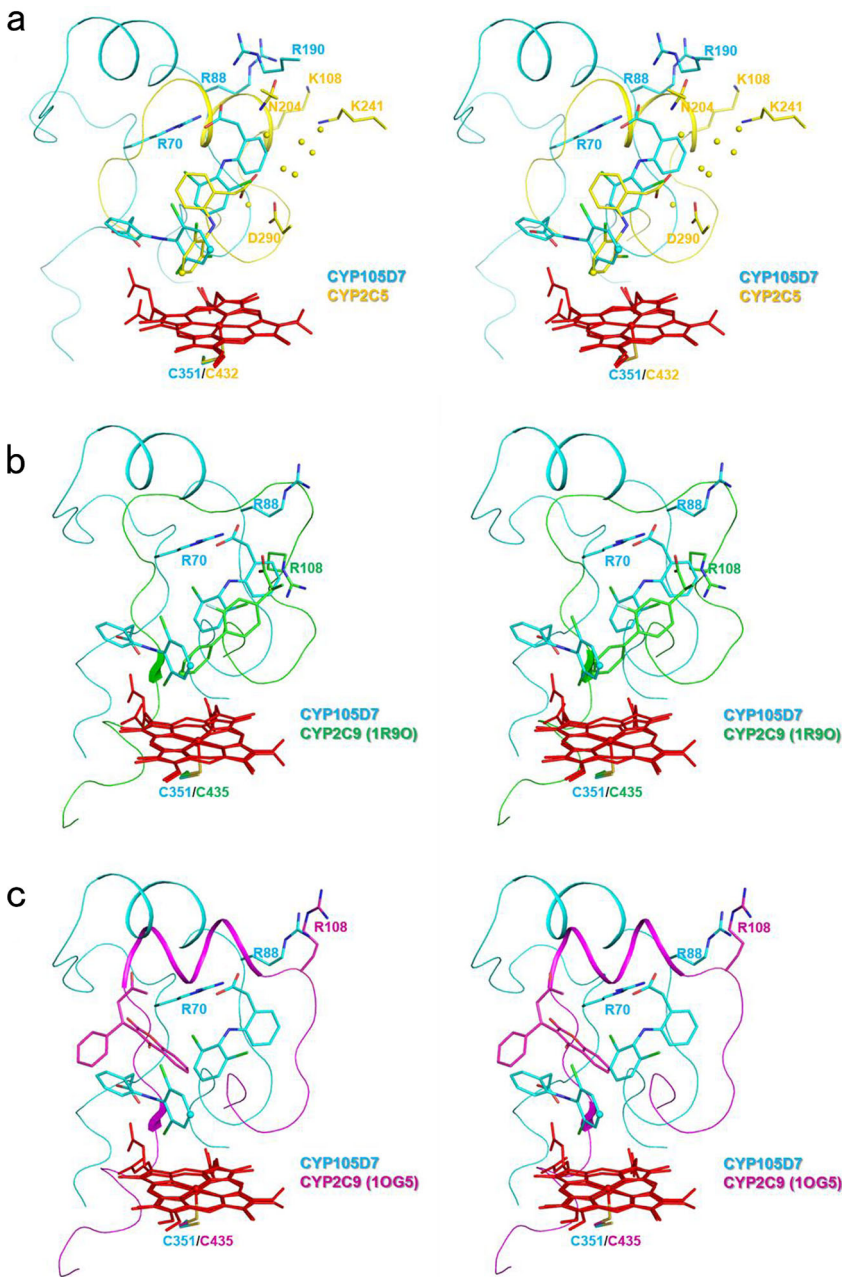

Fig. 5 Active site structures of CYP105D7–diclofenac (cyan) superimposed with CYP2C5 (**a**) and CYP2C9 (**b**, **c**). **a** CYP2C5 in complex with diclofenac (1NR6) is shown in *yellow*. **b**, **c** CYP2C9 in complex with flurbiprofen (1R9O) (**b**) and CYP2C9 with seven mutations in complex with *S*-warfarin (1OG5) (**c**) are shown in *green* and *magenta*, respectively. Water molecules and the hydroxylation target positions of the substrates are shown as *spheres*

of CYP2C9 (PDB code 1R9O) (Wester et al. 2004), in which the carboxylate side chain of flurbiprofen forms a salt bridge with Arg108 (Fig. 5b). The complex structure of CYP2C9 with diclofenac has not been reported, but Arg108 has been shown to play a key role in the hydroxylation function because substitution of this residue in CYP2C9 with other amino acids diminishes the activity of diclofenac (Dickmann et al. 2004; Ridderstrom et al. 2000). In the complex structure of CYP2C9 with *S*-warfarin using a construct with seven amino acid substitutions in the FG helix region (PDB code 1OG5), a large structural reorganization of the BC loop region places the Arg108 outside the active site (Williams et al. 2003) (Fig. 5c). The structural flexibility of the BC loop region may be required for the promiscuity of the drug-metabolizing enzyme. In the structure of CYP2C5, Lys108 is located in an "outside" position similar to that of the CYP2C9 in complex with *S*-warfarin (Fig. 5a). A basic residue (Arg or Lys) is highly conserved at this position (108) in various mammalian drug-metabolizing P450s, including CYP2C5, CYP2C9, CYP2C19, CYP2C8, CYP2D6, CYP2E1, and CYP2R1. In addition, another basic residue (Lys241) is involved in the indirect (water-mediated) recognition of the carboxylate of diclofenac in CYP2C5 (Fig. 5a). These basic residues could play important roles in recognition of substrates with anionic groups by promiscuous drug-metabolizing P450s. Interestingly, CYP105D7 also has three arginine residues (Arg70, Arg88, Arg190) at the distal side of the pocket (Fig. 5a). As discussed above, Arg70 directly recognizes the carboxylate of the distal diclofenac (DIF-2). The side chains of Arg88 and Arg190 are located outside the active site, but their positions correspond approximately to those of Arg108 in CYP2C9 (1OG5) and Lys108 in CYP2C5. Therefore, these arginine residues in CYP105D7 may also have a role in recognition of various substrates with a dynamic motion.

Recently, several structures of the CYP105 subfamily were determined, including those related to xenobiotic oxidation (CYP105A1 and CYP105AB3 as known as P450mox) (Sugimoto et al. 2008; Yasutake et al. 2007) and biosynthesis of secondary metabolites (CYP105P1, CYP105D6, CYP105N1) (Xu et al. 2009; Xu et al. 2010; Zhao et al. 2012b). Among them, complex structures with a substrate were determined for two P450s (CYP105A1 and CYP105P1). CYP105D7 and CYP105D6 belong to the same subfamily with high amino acid sequence identity (56 %), but their functions are completely different. The overall structure of the CYP105D7–diclofenac complex is similar to that of ligand-free structure of CYP105D6 (PDB code 3ABB; RMSD for 361 Cα atoms=2.0 Å). We could not directly compare the substrate recognition of these enzymes because the BC and FG loop regions in the CYP105D6 structure are disordered for 15 residues. However, the regions important for the ligand recognition of CYP105D7 (BC loop, FG helices, I

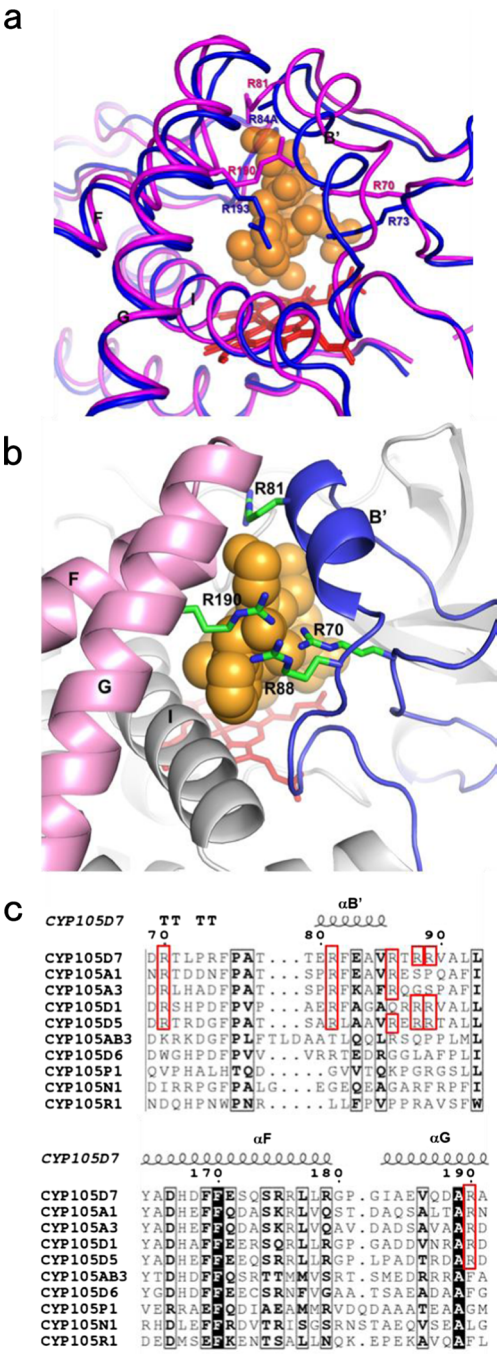

Fig. 6 Conserved arginine residues on the surface of an active site pocket. **a** Main chain traces of the CYP105D7–diclofenac complex (*magenta*) and CYP105A1 (2ZBZ, *blue*). The ligand molecule in CYP105D7 (DIF-1, DIF-2, PGE) is shown as an *orange sphere*. Arg70, Arg81, and Arg190 in CYP105D7 and corresponding amino acid residues in CYP105A1 structure are shown as *sticks*. **b** BC loop and FG helices of CYP105D7–diclofenac are shown in *blue* and *pink*, respectively. Ligand molecules (DIF-1, DIF-2) are shown as *orange spheres*, and arginine residues are shown as *green sticks*. **c** Amino acid sequence alignment at the BC loop and FG helix regions are shown. Secondary structures of CYP105D7 are indicated above the sequence. Completely and relatively conserved regions are highlighted by *black and white inverse characters and boxes*, respectively. Conserved arginine residues in the CYP105 family are shown as *red boxes*

helix, K/β6 strand, C-terminal loop region) shows low conservation with CYP105D6. Moreover, the residues involved in diclofenac binding (Arg70, Leu177, Leu178, Arg390) are not conserved at all, explaining why these P450s have distinct functions despite the high overall sequence similarity.

The crystal structure of CYP105A1 from *Streptomyces griseolus* in complex with 1α,25-dihydroxyvitamin D_3 ($1\alpha,25(OH)_2D_3$) has been reported (PDB code 3CV9) (Sugimoto et al. 2008). CYP105D7 and CYP105A1 do not belong to the same subfamily, but these two enzymes show 57 % amino acid sequence identity. The crystal structures of CYP105D7 and CYP105A1 are also very similar (RMSD= 1.2 Å). However, the pocket volume of CYP105D7 (2,037 $Å^3$) is much larger than that of CYP105A1 (1,537 $Å^3$). This is due to conformations of the FG region, the C-terminal loop, and BC loop regions of CYP105D7 because they are more open than those of CYP105A1 (Fig. 6a). The distal pocket of CYP105D7 contains four arginine residues (Arg70, Arg81, Arg88, Arg190) forming a wall of the substrate-binding pocket (Fig. 6b). This feature is similar to the CYP105A1 structure, in which the three arginine residues (Arg73, Arg84, Arg193) are important for binding activity and hydroxylation (Sugimoto et al. 2008). Other xenobiotics metabolizing P450s in the CYP105 family (CYP105A3 or P450sca; CYP105D1 or P450soy; CYP105D5) also have conserved arginine residues corresponding to Arg70, Arg81, and Arg190 in CYP105D7 (Fig. 6c). In particular, CYP105D1 and CYP105D5 have five or six arginine residues at positions 70, 81, 86, 88, 89, and 190. CYP105D1 and CYP105D5 have been studied as xenobiotics metabolizing P450s (Agematu et al. 2006; Chun et al. 2007; Taylor et al. 1999), but their crystal structures have not been reported. The residues important for recognition of the two diclofenac molecules are highly conserved in CYP105D1 and CYP105D5. Therefore, these three enzymes in the CYP105D family (D1, D5, D7) probably have similar function to hydroxylate various xenobiotic compounds. In contrast, for CYP105 family enzymes involved in the biosynthesis of secondary metabolites (CYP105D6, CYP105P1, CYP105N1, CYP105R1), the three arginine residues corresponding to Arg70, Arg81, and Arg190 in CYP105D7 are replaced with other amino acids (Fig. 6c).

In summary, xenobiotics metabolizing P450s have conserved arginine/lysine residues at the entrance of the substrate-binding pocket. However, importance of these residues remains to be verified. CYP105D7 can carry out the hydroxylation of various compounds that are used clinically, and this function is very similar to the human drug-metabolizing P450s. For industrial applications, bacterial P450s may be more suitable because they are soluble and easy for handing. So, CYP105D7 has a potential for application, e.g., regioselective or stereoselective introduction of a hydroxyl group into target molecules, and their metabolites may have potential for new drugs.

Acknowledgments We thank the staff of the Photon Factory for X-ray data collection. This work was supported by a Grant-in-Aid for Scientific Research from the Japan Society for the Promotion of Science. L-H.X. was supported by the fundamental research funds for the central universities (No. 2013QNA4042) and National Natural Science Foundation (No. 81402810).

References

Agematu H, Matsumoto N, Fujii Y, Kabumoto H, Machida K, Ishikawa J, Arisawa A (2006) Hydroxylation of testosterone by bacterial cytochromes P450 using the *Escherichia coli* expression system. Biosci Biotechnol Biochem 70:307–311

Bates PA, Kelley LA, MacCallum RM, Sternberg MJ (2001) Enhancement of protein modeling by human intervention in applying the automatic programs 3D-JIGSAW and 3D-PSSM. Protein Suppl 5:39–46

Bernhardt R, Urlacher VB (2014) Cytochromes P450 as promising catalysts for biotechnological application: chances and limitations. Appl Microbiol Biotechnol 98:6185–6203

Chun YJ, Shimada T, Sanchez-Ponce R, Martin MV, Lei L, Zhao B, Kelly SL, Waterman MR, Lamb DC, Guengerich FP (2007) Electron transport pathway for a *Streptomyces* cytochrome P450: cytochrome P450 105D5-catalyzed fatty acid hydroxylation in *Streptomyces coelicolor* A3(2). J Biol Chem 282:17486–17500

Cupp-Vickery J, Anderson R, Hatziris Z (2000) Crystal structures of ligand complexes of P450eryF exhibiting homotropic cooperativity. Proc Natl Acad Sci U S A 97:3050–3055

DeVore NM, Scott EE (2012) Nicotine and 4-(methylnitrosamino)-1-(3-pyridyl)-1-butanone binding and access channel in human cytochrome P450 2A6 and 2A13 enzymes. J Biol Chem 287:26576–26585

Dickmann LJ, Locuson CW, Jones JP, Rettie AE (2004) Differential roles of Arg97, Asp293, and Arg108 in enzyme stability and substrate specificity of CYP2C9. Mol Pharmacol 65:842–850

Dundas J, Ouyang Z, Tseng J, Binkowski A, Turpaz Y, Liang J (2006) CASTp: computed atlas of surface topography of proteins with structural and topographical mapping of functionally annotated residues. Nucleic Acid Res 34:W116–W118

Ekroos M, Sjögren T (2006) Structural basis for ligand promiscuity in cytochrome P450 3A4. Proc Natl Acad Sci U S A 103:13682–13687

Emsley P, Lohkamp B, Scott WG, Cowtan K (2010) Features and development of Coot. Acta Crystallogr D Biol Crystallogr 66:486–501

Fujita N, Sumisa F, Shindo K, Kabumoto H, Arisawa A, Ikenaga H, Misawa N (2009) Comparison of two vectors for functional expression of a bacterial cytochrome P450 gene in *Escherichia coli* using CYP153 genes. Biosci Biotechnol Biochem 73:1825–1830

Guengerich FP (2003) Cytochrome P450 oxidations in the generation of reactive electrophiles: epoxidation and related reactions. Arch Biochem Biophys 409:59–71

Hayashi K, Sugimoto H, Shinkyo R, Yamada M, Ikeda S, Ikushiro S, Kamakura M, Shiro Y, Sakaki T (2008) Structure-based design of a highly active vitamin D hydroxylase from *Streptomyces griseolus* CYP105A1. Biochemistry 47:11964–11972

Holm L, Sander C (1995) Dali: a network tool for protein structure comparison. Trends Biochem Sci 20:478–480

Johnson EF, Stout CD (2013) Structural diversity of eukaryotic membrane cytochrome P450s. J Biol Chem 288:17082–17090

Lamb DC, Skaug T, Song H-L, Jackson CJ, Podust LM, Waterman MR, Kell DB, Kelly DE, Kelly SL (2002) The cytochrome P450 complement (CYPome) of *Streptomyces coelicolor* A3 (2). J Biol Chem 277:24000–24005

Lamb DC, Waterman MR, Kelly SL, Guengerich FP (2007) Cytochromes P450 and drug discovery. Curr Opin Biotechnol 18: 504–512

Lamb DC, Waterman MR, Zhao B (2013) *Streptomyces* cytochromes P450: applications in drug metabolism. Expert Opin Drug Metab Toxicol 9:1279–1294

Lovell SC, Davis IW, Arendall WB, de Bakker PI, Word JM, Prisant MG, Richardson JS, Richardson DC (2003) Structure validation by Cα geometry: ϕ, ψ and Cβ deviation. Protein Struct Funct Bioinform 50:437–450

Mancy A, Antignac M, Minoletti C, Dijols S, Mouries V, Ha Duong N-T, Battioni P, Dansette PM, Mansuy D (1999) Diclofenac and its derivatives as tools for studying human cytochromes P450 active sites: particular efficiency and regioselectivity of P450 2Cs. Biochemistry 38:14264–14270

Munro AW, Girvan HM, Mason AE, Dunford AJ, McLean KJ (2013) What makes a P450 tick? Trends Biochem Sci 38:140–150

Murshudov GN, Vagin AA, Dodson EJ (1997) Refinement of macromolecular structures by the maximum-likelihood method. Acta Crystallogr D Biol Crystallogr 53:240–255

Ohyama K, Murayama N, Shimizu M, Yamazaki H (2014) Drug interactions of diclofenac and its oxidative metabolite with human liver microsomal cytochrome P450 1A2-dependent drug oxidation. Xenobiotica 44:10–16

Omura T, Sato R (1964) The carbon monoxide-binding pigment of liver microsomes: I evidence for its hemoprotein nature. J Biol Chem 239:2370–2378

Ortiz de Montellano PR (2005) Cytochrome P450: structure, mechanism, and biochemistry, 3rd edn. Kluwer Academic/Prenum Publishers, New York

Oshima R, Fushinobu S, Su F, Zhang L, Takaya N, Shoun H (2004) Structural evidence for direct hydride transfer from NADH to cytochrome P450nor. J Mol Biol 342:207–217

Otwinowski Z, Minor W (1997) Processing of X-ray diffraction data collected in oscillation mode. Methods Enzymol 276:307–326

Pandey BP, Roh C, Choi KY, Lee N, Kim EJ, Ko S, Kim T, Yun H, Kim BG (2010) Regioselective hydroxylation of daidzein using P450 (CYP105D7) from *Streptomyces avermitilis* MA4680. Biotechnol Bioeng 105:697–704

Prior JE, Shokati T, Christians U, Gill RT (2010) Identification and characterization of a bacterial cytochrome P450 for the metabolism of diclofenac. Appl Microbiol Biotechnol 85:625–633

Ridderstrom M, Masimirembwa C, Trump-Kallmeyer S, Ahlefelt M, Otter C, Andersson TB (2000) Arginines 97 and 108 in CYP2C9 are important determinants of the catalytic function. Biochem Biophys Res Commun 270:983–987

Sawada N, Sakaki T, Yoneda S, Kusudo T, Shinkyo R, Ohta M, Inouye K (2004) Conversion of vitamin D_3 to 1α, 25-dihydroxyvitamin D_3 by *Streptomyces griseolus* cytochrome P450SU-1. Biochem Biophys Res Commun 320:156–164

Schoch GA, Yano JK, Sansen S, Dansette PM, Stout CD, Johnson EF (2008) Determinants of cytochrome P450 2C8 substrate binding structures of complexes with montelukast, troglitazone, felodipine, and 9-cis-retinoic acid. J Biol Chem 283:17227–17237

Serizawa N, Matsuoka T (1991) A two component-type cytochrome P450 monooxygenase system in a prokaryote that catalyzes hydroxylation of ML-236B to pravastatin, a tissue-selective inhibitor of 3-hydroxy-3-methylglutaryl coenzyme A reductase. Biochim Biophys Acta 1084:35–40

Shen S, Marchick MR, Davis MR, Doss GA, Pohl LR (1999) Metabolic activation of diclofenac by human cytochrome P450 3A4: role of 5-hydroxydiclofenac. Chem Res Toxicol 12:214–222

Sugimoto H, Shinkyo R, Hayashi K, Yoneda S, Yamada M, Kamakura M, Ikushiro S-i, Shiro Y, Sakaki T (2008) Crystal structure of CYP105A1 (P450SU-1) in complex with 1α, 25-dihydroxyvitamin D_3. Biochemistry 47:4017–4027

Takamatsu S, Xu LH, Fushinobu S, Shoun H, Komatsu M, Cane DE, Ikeda H (2011) Pentalenic acid is a shunt metabolite in the biosynthesis of the pentalenolactone family of metabolites: hydroxylation of 1-deoxypentalenic acid mediated by CYP105D7 (SAV_7469) of *Streptomyces avermitilis*. J Antibiot (Tokyo) 64:65–71

Taylor M, Lamb DC, Cannell R, Dawson M, Kelly SL (1999) Cytochrome P450105D1 (CYP105D1) from *Streptomyces griseus*: heterologous expression, activity, and activation effects of multiple xenobiotics. Biochem Biophys Res Commun 263:838–842

Todd PA, Sorkin EM (1988) Diclofenac sodium. Drugs 35:244–285

Tsotsou GE, Sideri A, Goyal A, Di Nardo G, Gilardi G (2012) Identification of mutant Asp251Gly/Gln307His of cytochrome P450 BM3 for the generation of metabolites of diclofenac, ibuprofen and tolbutamide. Chem A Eur J 18:3582–3588

Urlacher VB, Girhard M (2012) Cytochrome P450 monooxygenases: an update on perspectives for synthetic application. Trends Biotechnol 30:26–36

Vagin A, Teplyakov A (1997) MOLREP: an automated program for molecular replacement. J Appl Crystallogr 30:1022–1025

Wester MR, Johnson EF, Marques-Soares C, Dijols S, Dansette PM, Mansuy D, Stout CD (2003) Structure of mammalian cytochrome P450 2C5 complexed with diclofenac at 2.1 Å resolution: evidence for an induced fit model of substrate binding. Biochemistry 42: 9335–9345

Wester MR, Yano JK, Schoch GA, Yang C, Griffin KJ, Stout CD, Johnson EF (2004) The structure of human cytochrome P450 2C9 complexed with flurbiprofen at 2.0-A resolution. J Biol Chem 279: 35630–35637

Williams PA, Cosme J, Ward A, Angove HC, Matak Vinkovic D, Jhoti H (2003) Crystal structure of human cytochrome P450 2C9 with bound warfarin. Nature 424:464–468

Xu L-H, Fushinobu S, Ikeda H, Wakagi T, Shoun H (2009) Crystal structures of cytochrome P450 105P1 from *Streptomyces avermitilis*: conformational flexibility and histidine ligation state. J Bacteriol 191:1211–1219

Xu L-H, Fushinobu S, Takamatsu S, Wakagi T, Ikeda H, Shoun H (2010) Regio-and stereospecificity of filipin hydroxylation sites revealed by crystal structures of cytochrome P450 105P1 and 105D6 from *Streptomyces avermitilis*. J Biol Chem 285:16844–16853

Yasutake Y, Imoto N, Fujii Y, Fujii T, Arisawa A, Tamura T (2007) Crystal structure of cytochrome P450 MoxA from *Nonomuraea recticatena* (CYP105). Biochem Biophys Res Commun 361:876–882

Zhao B, Lei L, Kagawa N, Sundaramoorthy M, Banerjee S, Nagy LD, Guengerich FP, Waterman MR (2012a) Three-dimensional structure of steroid 21-hydroxylase (cytochrome P450 21A2) with two substrates reveals locations of disease-associated variants. J Biol Chem 287:10613–10622

Zhao B, Moody SC, Hider RC, Lei L, Kelly SL, Waterman MR, Lamb DC (2012b) Structural analysis of cytochrome P450 105N1 involved in the biosynthesis of the Zincophore, Coelibactin. Int J Mol Sci 13:8500–8513